ACS Synthetic Biology

pubs.acs.org/synthbio

Research Article

CTRL Enables Gene-Specific RNA Regulation Using CRISPR-Cas7−11

Tianqi Wang, Daniel J. Brogan, Natalie M. Zawalick, Fangying Chen, Yeran Mkrtchian, Alexis C. Komor, and Omar S. Akbari*

Cite This: https://doi.org/10.1021/acssynbio.5c00658

Read Online

ACCESS | Metrics & More | Article Recommendations | Supporting Information

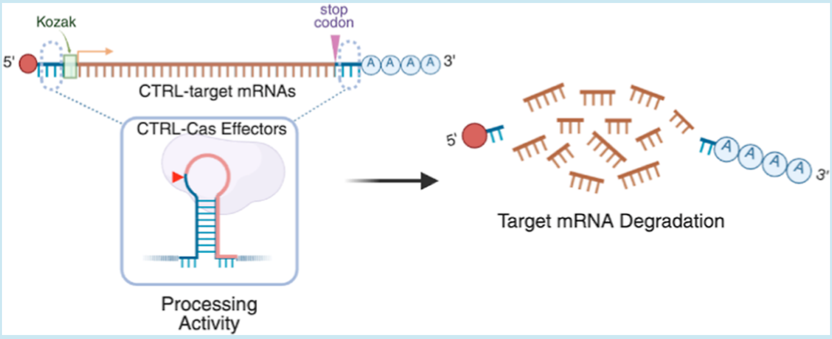

ABSTRACT: Advancements in synthetic biology have enabled the development of precision gene expression technologies for comprehensive investigations of biological and biochemical networks. Here, we describe the development of a refined and innovative tool, CRISPR-Cas Transgenic Repressible eLement (CTRL), which utilizes the direct repeat processing activity of the recently discovered CRISPR-Cas7−11 effector to site-specifically target synthetic mRNA molecules. We demonstrate that CTRL exhibits high efficiency, tunable regulation of expression, and gene-specific repression of mRNA and protein expression. We engineered multiple permutations of the Cas7−11 effector that differ in their ability to reduce gene expression, suggesting flexibility for the application of choice. CTRL is a novel variation on gene repression technology that exhibits broad applicability across multiple model systems.

KEYWORDS: *gene regulation, gene expression, CRISPR-Cas, gene circuit, RNA-targeting, synthetic biology, CRISPR-Cas engineering, Cas7−11, gRAMP*

■ INTRODUCTION

Gene knockdown enables the characterization of gene expression, signaling pathways, and molecular interactions. The discovery of RNA-targeting CRISPR-Cas systems[1] has enabled the development of programmable RNA-targeting systems for effective gene knockdown. RNA-targeting CRISPR-Cas systems are categorized as either type III or type VI (Cas13), where type III systems predominantly utilize multisubunit effectors[2,3] and type VI systems encode a single polypeptide.[4] Robust RNA knockdown has been achieved with multiple type III[5,6] and type VI systems.[7−9] These systems can theoretically target any gene of interest, but the on-target efficacy is variable and requires large screens to optimize gRNA design.[10,11] Cas13 also exhibits a nonspecific RNase activity useful for diagnostics[12−14] but can have toxic off−target activity.[15−18] These characteristics limit the precision of gene knockdown at the post-transcriptional level and present an opportunity to develop improved gene knockdown technologies.

RNA-targeting CRISPR-Cas systems possess two different RNase activities: target cleavage and CRISPR-RNA (crRNA) array processing.[6,19,20] Target cleavage is accomplished through ternary complex formation, where the spacer hybridizes with its complement and utilizes divalent cations to coordinate catalysis.[21−23] However, crRNA array processing operates independently of metal ions. crRNA array processing occurs when a CRISPR effector recognizes the distinct sequence and secondary structure of the crRNA direct repeat (DR) and cuts the 5′ and/or 3′ end of the crRNA, resulting in a mature crRNA molecule. crRNA array processing is consistent regardless of the programmed spacer and, therefore differs from target cleavage, which is inherently variable across targets.[24] Due to the variability of target cleavage, we sought to develop a generalizable RNA-targeting system that utilizes the consistent crRNA array processing activity of type III-E Cas enzymes, or Cas7−11 proteins.

Received: September 3, 2025
Revised: October 21, 2025
Accepted: November 3, 2025

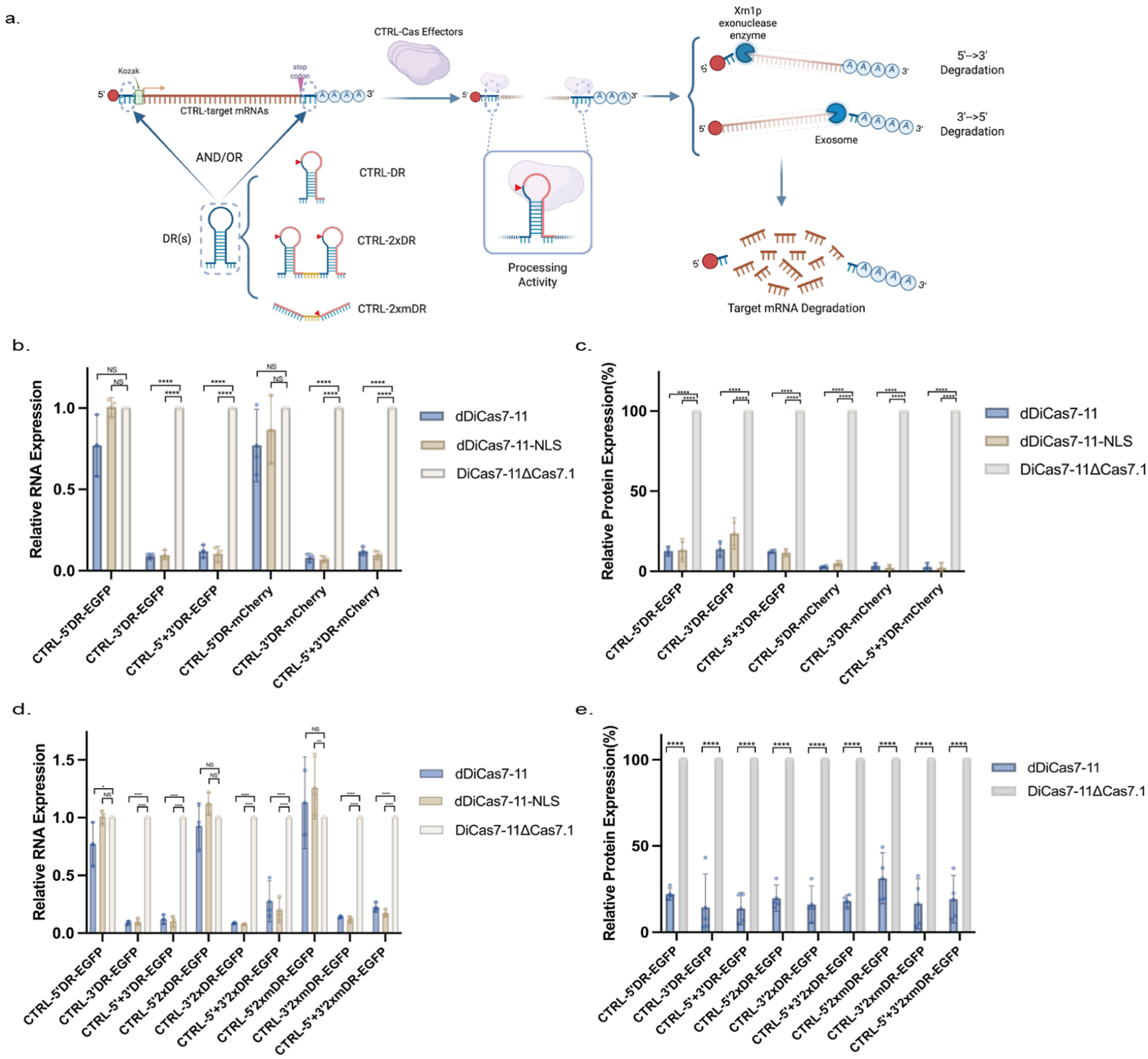

Figure 1. CTRL construction, experimental design, and results of initial screening on variant CTRL constructs. (a) Schematic representation of CTRL-DR design and processing. The dashed line ovals show the direct repeats (DRs) insertion sites. The red triangle indicates the processing site on the DRs. The processed mature DRs are indicated in red. (b) qPCR analysis of CTRL-DR-EGFP/mCherry RNA knockdown with dDiCas7−11 (F (6, 14) = 38.64, $P < 0.0001$) and dDiCas7−11-NLS (F (6, 14) = 88.00, $P < 0.0001$) at a CTRL-effector:reporter molar ratio of 15:1 (Table S3). Error bars represent SEM (n = 3). (c) Flow cytometry analysis of CTRL-DR-EGFP/mCherry protein knockdown with full-length dDiCas7−11(F (6, 7) = 342.7, $P < 0.0001$) and dDiCas7−11-NLS (F (6, 7) = 100.1, $P < 0.0001$) at a CTRL-effector:reporter molar ratio of 15:1 (Table S3). Error bars represent SEM (n = 3). (d) qPCR analysis of the RNA expression of CTRL-EGFP constructs engineered with unprocessed DRs (CTRL-2xDR) or processed (or mature) DRs (CTRL-2xmDR) and full-length dDiCas7−11 (F (9, 19) = 24.71, $P < 0.0001$) and dDiCas7−11-NLS (F (9, 20) = 75.81, $P < 0.0001$) at a 15:1 CTRL-effector:reporter molar ratio (Table S3). Error bars represent SEM (n = 3). (e) Flow cytometry protein expression analysis of CTRL-2xDR-EGFP and CTRL-2xmDR-EGFP constructs and full-length dDiCas7−11 (F (9, 30) = 21.28, $P < 0.0001$) at a 10:1 CTRL-effector:reporter molar ratio (Table S3). Error bars represent SEM (n = 4). For each analysis, significant differences in protein or RNA expression were determined by a one-way ANOVA and a Dunnett's multiple comparisons test between the CTRL-effectors and the DiCas7−11ΔCas7.1 control. P value style = GP (NS: $P \geq 0.05$; *: $P < 0.05$; **: $P < 0.01$; ***: $P < 0.001$; ****: $P < 0.0001$).

Here, we repurpose the crRNA processing activity of the recently discovered type III-E effectors (Cas7−11)[6,25] to develop a genetic tool for gene-specific knockdown, CRISPR-Cas Transgenic Repressible eLement (CTRL). Some class 2 CRISPR systems, such as Cas12 or Cas13 are capable of processing their own crRNA arrays, but their nucleic acid binding capabilities remain active.[26] However, Cas7−11 can be truncated down to the single array processing domain, Cas7.1, providing a small RNase domain capable of recognizing a specific RNA sequence and structure, similar to other class 1 crRNA array processing enzymes,[27,28] while retaining the possibility of being further engineered with the native sequence of Cas7−11. We demonstrate the efficacy of CTRL by encoding multiple permutations of crRNA DRs into mRNA

https://doi.org/10.1021/acssynbio.5c00658
ACS Synth. Biol. XXXX, XXX, XXX−XXX

molecules to identify the minimal DR sequence required for robust gene knockdown. We show that CTRL is capable of both transcriptional and translational repression and can regulate the downstream activity of enzymes such as CRISPR-Cas9. We also demonstrate titration of CTRL effectors results in a range of effectiveness facilitating tunable gene knockdown and making it a powerful tool for modeling variable gene expression.

■ RESULTS

CTRL is Capable of Effective RNA and Protein Downregulation. To determine if CTRL can effectively downregulate protein expression, we designed constructs with crRNA DRs encoded at the 5′ and/or 3′ end of the target coding sequence for the gene of interest (Figure 1a). The 5′ DRs were encoded downstream of the CMV promoter, but upstream of the Kozak sequence and start codon, whereas the 3′ DRs were encoded downstream of the stop codon but upstream of the polyA signal (Figures 1a and S1). Previous studies demonstrated that DiCas7−11 can efficiently process the 5′ DR of pre-crRNA molecules into mature crRNAs.[6] We hypothesized that DiCas7−11-based effectors could process the DRs encoded in a transcribed construct and remove either the 5′ cap and/or the 3′ poly-A tail depending on the DR placement. To support strict crRNA processing and avoid nonspecific cleavage, we catalytically inactivated target cleavage for the Cas7−11 constructs (dDiCas7−11) (Figure S1). Additionally, the Cas7.1 domain is solely responsible for crRNA processing in Cas7−11 proteins,[23,29] and we, therefore, established a Cas7.1 deletion mutant (DiCas7−11ΔCas7.1) as a negative control effector in this study (Figure S1). Following DR processing, we hypothesized that the targeted mRNAs would be degraded by the endogenous cell machinery,[30] thus allowing for transient regulation of both mRNA and protein expression.

We developed EGFP- and mCherry-reporter assays to assess the efficacy of the CTRL system, evaluating their mRNA and protein expression using RT-qPCR and flow cytometry, respectively (Figure S2). The initial EGFP- and mCherry-reporter screens consisted of three different constructs encoding a single 35nt unprocessed direct repeat (CTRL-DR) at the 5′, the 3′ end, or both the 5′/3′ ends of the EGFP or mCherry transcript (Figure S1). In both reporter assays, with the dDiCas7−11 construct, we observed over 90% reduction in RNA expression in constructs with a DR encoded at the 3′ end or both the 3′/5′ ends of the transcript, while almost no knockdown was observed with a DR at the 5′ end only, as compared to the negative control effector DiCas7−11ΔCas7.1 (Figure 1b). Similar results were obtained with targeting unmodified EGFP and mCherry proteins as the negative control groups (Figure S3a,b). However, the flow cytometry data revealed that EGFP and mCherry protein expression was reduced by >80% in all constructs, including the 5′ encoded DR (Figure 1c). We also hypothesized that fusing a Nuclear Localization Signal (NLS) to the Cas7−11 protein would result in earlier RNA processing and therefore, greater gene knockdown. However, the addition of an NLS did not significantly improve repression by CTRL (Figure 1b,c). We speculate that cytoplasmic targeting of the mRNA is already sufficient, such that increasing nuclear localization for pre-mRNA cleavage does not further boost repression activity.

CTRL has Flexible Design Criteria and is Effective at Low Molar Ratios. Next, we expanded our design strategy to improve and achieve consistent RNA and protein knockdown efficiency. We explored alternative DRs in the EGFP-reporter constructs and generated constructs with double unprocessed DRs (CTRL-2xDR) and double processed (or mature) DRs (CTRL-2xmDR) (Figures 1a and S1) at the 5′, 3′, or both the 5′/3′ ends of the transcript. Prior reports demonstrated that Cas7−11 proteins can recognize and cleave the mature DRs.[31,32] Aside from the constructs with DRs encoded at the 5′ end, we observed 80%−90% RNA knockdown for all other constructs with no significant differences in knockdown between designs ($F(5, 12) = 0.02110$, $P = 0.9998$) (Figure 1d). However, there was a substantial reduction (70−85%) in EGFP protein levels for all constructs, including 5′ encoded DRs ($F\ (9, 30) = 21.28$, $P < 0.0001$) (Figure 1e). The lower protein knockdown compared to RNA may reflect saturation of translation in control groups, which limits proportional changes in protein expression when reductions are measured relative to control levels.

To reconcile the differences in protein and RNA knockdown with 5′ encoded DRs, we performed RT-qPCR analysis with three primer pairs: F2-R2 and F3-R3, that detected transcripts within the EGFP-reporter coding sequence; and F1-R1, which amplifies around the DRs at the 5′ end of the transcript (Figure S4a). The relative RNA expression in the EGFP coding region did not indicate RNA knockdown, but the mRNA level of the 5′ DR reduced by 40−70% (Figure S4b−d). These data suggest that the 5′ DRs were processed, but the transcripts were not degraded. Therefore, this approach reduces protein expression but does not result in the turnover of the targeted mRNA molecule.

Prior assays were conducted at an Effector-to-Reporter molar ratio (Effector/Reporter) of 15:1. To evaluate the protein knockdown capabilities at lower Effector/Reporter ratios, we lowered the effective ratio from 15:1 to 10:1 and conducted the same flow cytometry analysis for all 9 designs. The protein levels decreased by 70−80%, which was approximately 10% less reduction in protein expression than with a higher molar ratio, and again, we observed no significant difference in overall protein knockdown across all designs (Figure 1e). Therefore, we selected the 3′ CTRL-2xmDR design for all subsequent assays. This construct design is minimal, encodes two processing sites, and achieves consistent RNA and protein downregulation.

A C-Terminal Truncation of the Cas7−11 Protein Effectively Reduces Gene Expression. Previous studies have demonstrated that Cas7−11 proteins only require the Cas7.1 domain to process the 5′ DR in CRISPR arrays.[29] The Cas7.2 domain helps anchor the pre-crRNA in DR processing which suggests that the Cas7.2 domain enhances crRNA processing.[23,33] Therefore, we created two truncated DiCas7−11 proteins to test in the CTRL system: (1) a complete truncation from the C-terminus leaving only the Cas7.1 domain (Cas7.1, and 2) a partial C-terminal truncation with intact Cas7.1, and Cas11 domains, an inactive Cas7.2 domain, and the linkers in between the domains (Cas7.1−7.2) (Figure S1, Table S3). These truncated wild-type DiCas7−11 variants are incapable of crRNA-dependent target binding or cleavage and are, therefore, specific to DR processing. Both Cas7.1 and Cas7.1−7.2 significantly repressed mRNA expression of all 9 CTRL-DR(s)-EGFP constructs, indicating that the truncation did not abolish their processing activities (Figure S5).

To distinguish the repression efficiencies of all CTRL-effectors, we performed an Effector/Reporter molar ratio

https://doi.org/10.1021/acssynbio.5c00658
ACS Synth. Biol. XXXX, XXX, XXX−XXX

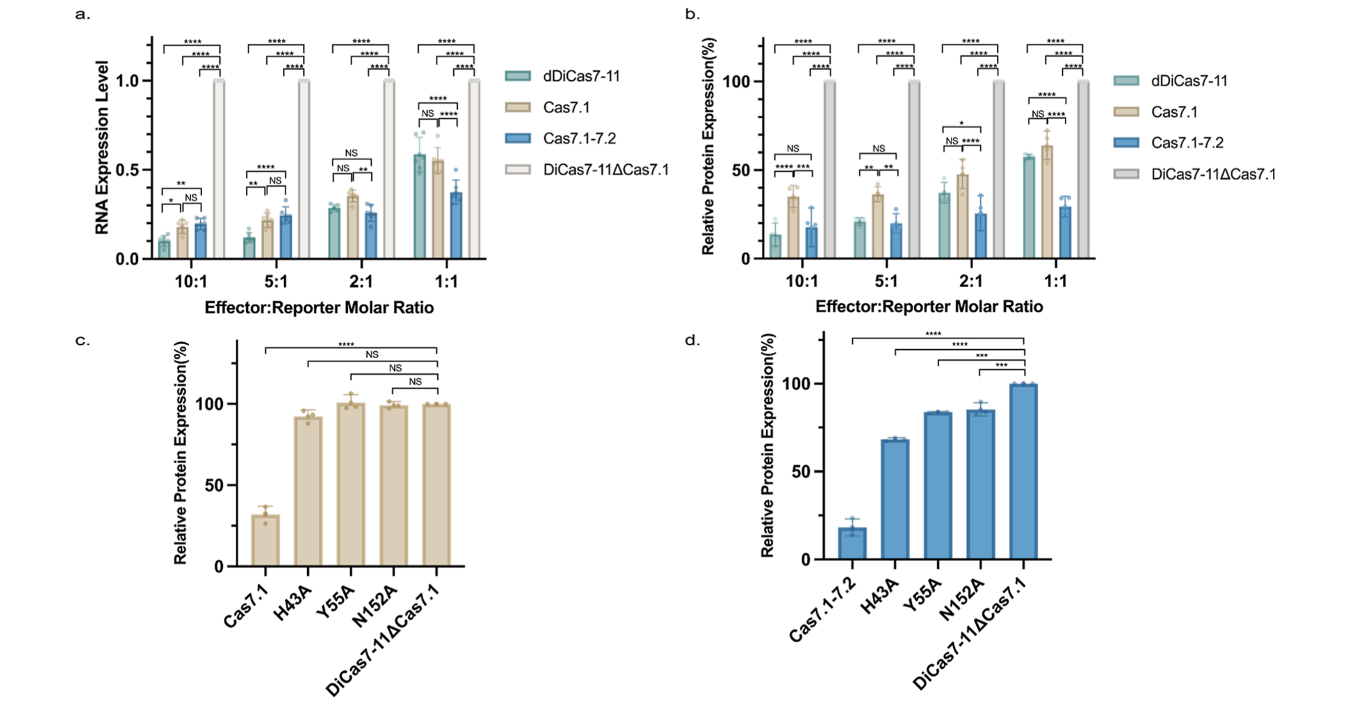

Figure 2. Titration assays of truncated CTRL-effectors and mechanistic evidence in CTRL. (a) qPCR analysis of RNA expression in the truncated and full-length CTRL-effectors at different CTRL-effector:reporter molar ratios (10:1, 5:1, 2:1, 1:1) (Table S3). (b) Flow cytometry analysis of protein expression in the truncated and full-length CTRL-effectors at different CTRL-effector:reporter molar ratios (10:1, 5:1, 2:1, 1:1) (Table S3). (c-d) Flow cytometry analysis of protein expression from mutated (c) Cas7.1 or (d) Cas7.1−7.2 with mutations in key residues (H43, Y55, N152) essential processing activities (Table S3). Significant differences in RNA expression were determined using one-way ANOVA, Dunnett's multiple comparisons test, and Tukey's multiple comparisons test. Error bars represent SEM (n = 4−6). P value style = GP (NS: $P \geq 0.05$; *: $P < 0.05$; **: $P < 0.01$; ***: $P < 0.001$; ****: $P < 0.0001$).

titration assay from 1:1 to 10:1. We observed a reduction in EGFP RNA and protein levels for all truncated CTRL-effectors tested, with repression increasing with the Effector/Reporter ratio (Figures 2a,b and S6a). At high molar ratios (10:1 and 5:1), the full-length dDiCas7−11 protein exhibited the highest protein and RNA knockdown (Figure 2a,b). However, the Cas7.1-Cas7.2 truncated construct outperformed all other CTRL-effectors at the lower molar ratios (1:1) (Figure 2a,b), only losing 20% of its maximum activity. The protein repression levels did not yield significant variance among different molar ratios (F (3, 12) = 1.602, P = 0.2407) (Table S3), indicating that the Cas7.1−7.2 variant is more effective at reducing protein expression on a mole-*per*-mole basis. The full-length Cas7−11 protein was very sensitive to Effector/Reporter ratios, where a 50% decrease in activity was observed at the lower molar ratios (Figure 2a,b). Interestingly, the Cas7.1 domain exhibited an Effector/Reporter ratio-dependent loss in activity similar to the full-length protein and resulted in significantly more EGFP protein expression than Cas7−11 or Cas7.1−7.2 at all molar ratios (Figure 2a,b).

Next we aimed to confirm whether the gene expression activity was strictly due to DR processing activities of our CTRL effectors. We mutated three previously identified residues in the Cas7.1 active site to alanine (H43A, Y55A, and N152A),[23] to generate Cas7−11 mutants incapable of processing DRs. We found that mutations in any of the three active site residues in Cas7.1 restored EGFP protein expression (F (3, 8) = 3.923, P = 0.0542) (Figure 2c, Table S3). Mutations in the Cas7.1-Cas7.2 protein, however, still had significantly reduced EGFP protein expression compared to the DiCas7−11ΔCas7.1 control (F (4, 10) = 387.5, P < 0.0001), but protein expression was significantly higher than the unmutated Cas7.1−7.2 construct (F (3, 8) = 305.5, P < 0.0001) (Figure 2d). Although Kato et al. reported complete loss of crRNA processing activity with H43A mutant and reduced activities with Y55A and N152A,[23] our results indicated an inverse pattern that the H43A mutant retained the most protein knockdown of all mutants (Figure 2d). Together, these results suggest that C-terminal truncations of Cas7−11 proteins are capable of crRNA processing, the inclusion of Cas11 and Cas7.2 domains improves the efficacy of CTRL at lower molar ratios, and the protein expression is strictly driven by Cas7.1-dependent DR processing activity.

CTRL Regulates the Endonuclease Activity of Cas9 and CasRx. With evidence of RNA and protein regulation by CTRL, we aimed to demonstrate that CTRL effectors can regulate the activity of a downstream target gene. We used toxin-like systems, and tested whether CTRL could regulate the activity of two CRISPR-Cas editors, SpyCas9-NG[34] and RfxCas13d (CasRx).[35] We cotransfected HEK cells with (1) a SpyCas9-NG plasmid including the CTRL-2xmDR at the 3′ end and the HEK293-site-3 sgRNA[36] sequence; and (2) a CTRL-effector plasmid (Figures 3a and S1). We simultaneously transfected SpyCas9-NG plasmids with CTRL-effector plasmids at a ratio of 15:1 and performed amplicon sequencing to analyze the indels generated for each condition. To maintain consistent transfection conditions across all groups, we used DiCas7−11ΔCas7.1 as the effector in the control group rather than excluding the effector entirely. CTRL-effectors reduced SpyCas9-NG indel formation at HEK293-site-3 by 27−50% compared to controls, from 31 to 34% to 17−21% (Figure 3b). Of all effectors tested, Cas7.1−7.2 was the most effective and

https://doi.org/10.1021/acssynbio.5c00658
ACS Synth. Biol. XXXX, XXX, XXX−XXX

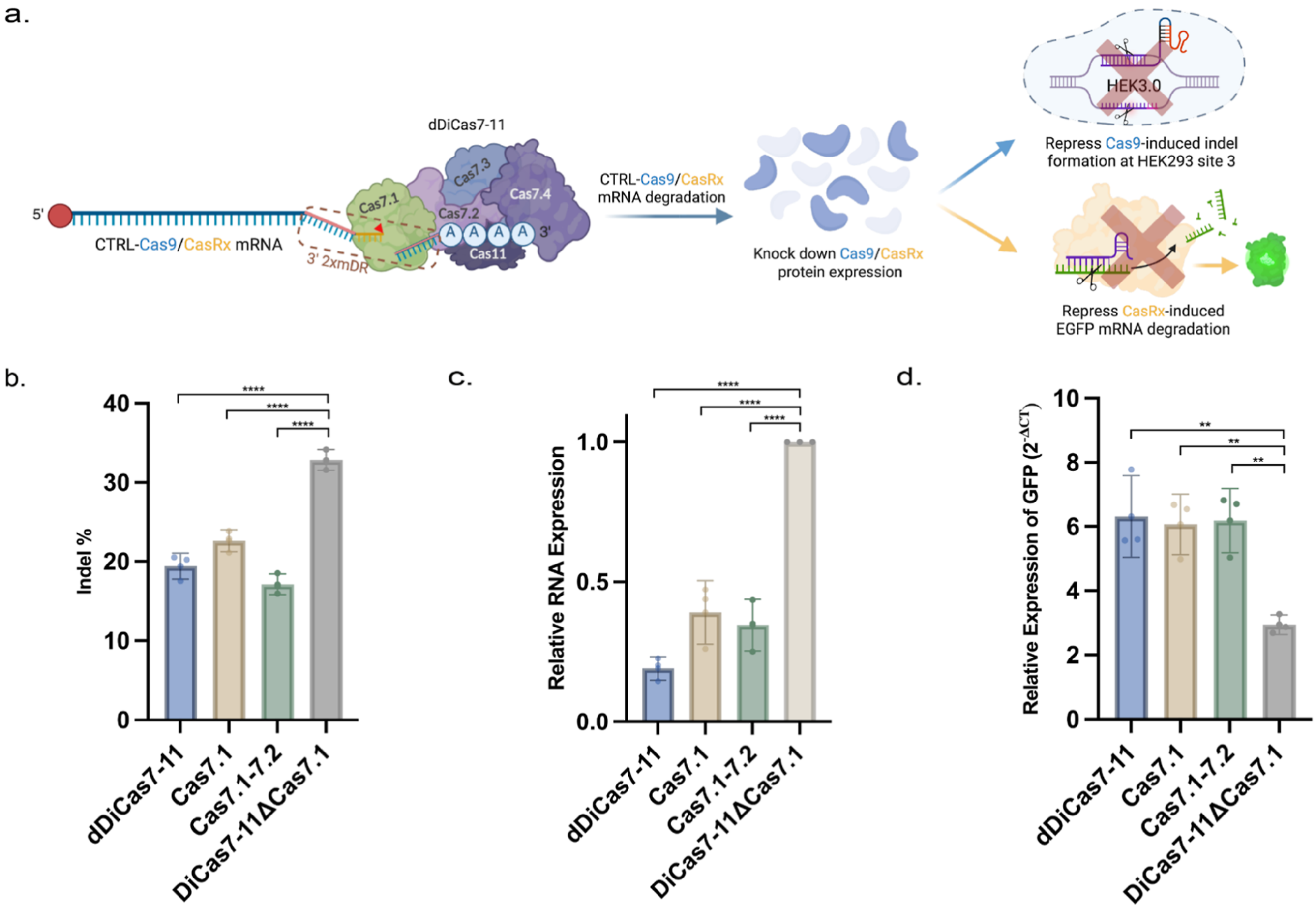

Figure 3. CTRL regulated SpyCas9-NG and CasRx endonuclease activities. (a) Schematic of the CTRL knockdown of SpyCas9-NG and CasRx cleavage activity. The red arrow indicates the processing site in the mDR sequence inserted downstream of the coding domain of SpyCas9-NG and CasRx. (b) Next-generation amplicon sequencing assessing SpyCas9-NG cleavage activity with CTRL effectors at a 15:1 CTRL-effector:CTRL-Cas9 molar ratio. The percentage of indels (insertions, deletions, and substitutions) within 8bp spanning the predicted cleavage site was generated by MiSeq high-throughput DNA sequencer (Illumina) and analyzed with CRISPResso2. Error bars represent SEM (n = 3). (c) qPCR assessing SpyCas9-NG mRNA expression by CTRL at a 15:1 CTRL-effector:CTRL-Cas9 molar ratio. Error bars represent SEM (n = 3). (c) Assessing CasRx cleavage activity (targeting EGFP) by CTRL via qPCR analysis of EGFP mRNA expression. The CTRL-effector:CTRL-CasRx molar ratio is 15:1. Error bars represent SEM (n = 3). Significant differences between all groups were calculated by one-way ANOVA and Dunnett's multiple comparisons test.

reduced SpyCas9-NG indel formation in half. The full-length dDiCas7−11 and Cas7.1 truncated proteins reduced indel formation by approximately 40% and 30%, respectively, indicating these CTRL permutations are much weaker regulators of target gene expression (Table S4).

Since indel formation only captures downstream CTRL effects, we also quantified SpyCas9-NG mRNA expression by qPCR. Interestingly, the full-length dDiCas7−11 protein exhibited the largest SpyCas9-NG mRNA knockdown (80%), while Cas7.1 and Cas7.1−7.2 only reduced mRNA expression by around 60−65% (Figure 3c). This result suggests that mRNA knockdown alone does not dictate how effective each CTRL variant will be at reducing the enzymatic activity of SpyCas9-NG.

Next, we assessed the ability of CTRL to regulate CasRx-mediated RNA knockdown. Identical to the design of SpyCas9-NG, we encoded the CTRL-2xmDR at the 3′ end of the CasRx coding sequence and cotransfected it with CTRL-effector plasmids, EGFP-targeting sgRNA plasmid, and EGFP-expressing plasmid (Figure 3a, S1). By competitively targeting CasRx with CTRL, we hypothesized we could restore EGFP expression. All three CTRL-effector permutations effectively reduced CasRx expression, increasing EGFP RNA expression 2-fold (Figures 3d and S6b). Together, these results demonstrate that CTRL can regulate the activity of enzymes that induce both permanent and transient changes in gene expression.

DISCUSSION

CTRL enables tunable expression of target genes of interest. By synthetically encoding Cas7−11 crRNA DRs, we demonstrated that CTRL enables robust, gene-specific knock-down. Using permutations of Cas7−11 and variably encoded DRs, we identified a potent but minimal system for gene expression control. We demonstrate that CTRL can regulate mRNA and protein expression at a range of concentrations but ultimately resulted in a 2-fold reduction in expression on an equimolar basis. We also showed that encoding CTRL into SpyCas9-NG or CasRx mRNA results in reduced nuclease activity in these potent enzymes. Overall, CTRL is an effective synthetic technology that can theoretically be applied to regulate gene expression for any gene of interest.

https://doi.org/10.1021/acssynbio.5c00658
ACS Synth. Biol. XXXX, XXX, XXX−XXX

We observed that positioning the DR at the 5′ end did not lead to mRNA degradation when using full-length Cas7−11 effectors, even though DR processing activity persisted (Figures 1b,d and S4). In contrast, truncated effectors such as Cas7.1 induced clear mRNA knockdown for the CTRL-5′2xDR/mDR-EGFP constructs (Figure S7). We speculate that this difference arises from structural interactions between the Cas7−11 effector and its RNA target. When the DR is located at the 5′ end, the full length Cas7−11 effector engages both the DR and the downstream mRNA sequence treating it as a spacer, which is recognized by Cas7.2-Cas7.4 and INS domains,[23] and inhibits endogenous ribonuclease activity to turnover the target mRNA. Conversely, when the DR is positioned at the 3′ end of the target transcript—or when only the Cas7.1 domain is present—Cas7−11 binding does not obstruct access to the terminal end of the mRNA, permitting degradation from both directions. This mechanistic interpretation remains speculative and requires further validation through structural analysis of Cas7−11−RNA complexes.

We observed less efficient repression of SpyCas9-NG and CasRx compared to EGFP and mCherry reporters, highlighting directions for improvement. Permutations of CTRL-Cas7−11 may express and fold at different rates that may be too slow to completely repress SpyCas9-NG or CasRx activity. For example, for SpyCas9-NG regulation, the full-length CTRL-dDiCas7−11 was the most effective at reducing mRNA expression; however, the CTRL-Cas7.1−7.2 effector had the greatest reduction in indel formation. Since Cas7.1−7.2 is smaller than dDiCas7−11, the rate at which the enzyme is produced and folds into its active state may be significantly faster than its full-length counterpart. Smaller enzymes may more rapidly impact mRNA expression and, ultimately, the protein expression of SpyCas9-NG. However, we cannot rule out that there may also be a mechanistic driver for this increase in activity that was not uncovered in this current study. Developing CTRL into an inducible system may improve the system's ability to precisely regulate gene expression by providing temporal control of the gene regulator.

CTRL may also be useful for therapeutic applications requiring precise control over timing and dosage.[37] Some synthetic tools refine genetic transcription by regulating transcription factors, which are difficult to control and monitor,[38] or by engineering enzymes, promoters, and terminators, which often lack precision and are not trivial to engineer.[39,40] CTRL enables precise and tunable gene expression regulation of both mRNA and protein, supporting multiple applications (Figure S8). CTRL targets and effectors require minimal design and engineering while achieving high efficiency regulating gene expression compared to spacer-based targeting, a reported limitation of CRISPR interference (CRISPRi) due to its slow kinetics.[38−40] CTRL may also provide a valuable alternative for generating synthetic toxin systems frequently used in genetic population control strategies, such as the Release of Insects Carrying a Dominant Lethal Gene (RIDL)[41] (Figure S8). Current approaches using antibiotics require careful evaluation and dose adjustment.[42] CTRL can potentially replace antibiotics to suppress toxin expression, minimizing toxicity and maintaining requirements, which can easily be removed through genetic crosses as well.

Altogether, CTRL has the potential for a broad range of applications, and this initial characterization demonstrates a high level of efficacy built into a robust system. A limitation of this study is that the CTRL system was evaluated exclusively in HEK293T cells, leaving its generalizability to other cellular contexts and in vivo models to be determined. With further development, particularly through integration with other advanced technologies, such as prime editing,[43] CTRL can expand its utility across various genomic and cellular contexts. Such advancements may facilitate the innovation of prior technologies, advancing both foundational research and translational applications in synthetic biology.

METHODS

Construct Design and Cloning. All plasmids were generated using the standard Gibson assembly methods. The reporter and effector expression plasmid were designed to contain the CMV promoter and the bovine growth hormone (bGH) terminator. The 5′ DRs were encoded downstream of the CMV promoter, but upstream of the Kozak sequence and start codon, whereas the 3′ DRs were encoded downstream of the stop codon (Figures 1a and S1). The inactivated Cas7−11 constructs were generated by mutating the active residues in the Cas7.2 and Cas7.3 domains (D429A/D654A).[23] All plasmids generated are available at Addgene (Figure S1).

Cell Culture Assays. All experiments used HEK293T cell lines obtained from the American Type Culture Collection (ATCC CRL-3216). The cells are incubated at 37 °C and 5% CO_2. For all cell experiments except for the Cas9 repression assay, the HEK293T cells were cultured in Dulbecco's Modified Eagle Medium (DMEM) (Thermo Fisher Scientific 11995073) with 10% Fetal Bovine Serum (FBS) (Corning 35−011-CV) and 1% penicillin−streptomycin (Thermo Fisher Scientific 15070063). 3.2×10^4 cells were seeded in a 48-well dish approximately 22 h before transfection, ensuring that their confluency was less than 60%. Transient transfections were carried out with Lipofectamine 3000 (Thermo Fisher Scientific L3000001) per the manufacturer's protocol. The HEK293T cells were cotransfected with 20 ng EGFP/mCherry CTRL-Reporter plasmids and the quantity of Cas7−11-based effector plasmids for the intended molar ratio. They were incubated for 48 h before harvesting for experiments.

For the SpyCas9-NG expression assay, the cells were cultured in DMEM with 10% FBS, without antibiotics (penicillin−streptomycin). 5.0×10^4 cells were seeded in a 48-well plate 24 h before transfection, and the transient transfections were conducted with Lipofectamine 2000 (Thermo Fisher Scientific 11668030) based on the manufacturer's protocol. They were harvested 72 h after transient transfection, and the culture media was changed once 48 h after the transfection.

qPCR and Data Analysis for RNA Expression. Cells were removed from the 48-well plate with 250 μL of RNAprotect Cell Reagent (Qiagen 76104) 48 h after transfection and stored at −20 °C for at least 24 h prior to extraction. Cells were lysed using QIAshredder (Qiagen 79656), and total RNA was then extracted using the RNeasy Mini Kit (Qiagen 74106) based on the manufacturer's protocol. The total RNA was treated with DNase (Thermo Fisher Scientific AM1907) to remove any remaining DNA. The concentration of the RNA samples was measured using a Nanodrop OneC UV−vis spectrophotometer (Thermo Fisher Scientific NDONEC-W). Approximately 0.75 μg of total RNA was used to synthesize cDNA with a RevertAid First Strand cDNA Synthesis Kit (Thermo Fisher Scientific K1622). cDNA was diluted (1:1000) for qPCR analysis. qPCR was performed with SYBR green (qPCRBIO SyGreen Blue Mix Separate-ROX

https://doi.org/10.1021/acssynbio.5c00658
ACS Synth. Biol. XXXX, XXX, XXX−XXX

17-507B, Genesee Scientific), using 4 μL of dilute cDNA in each 20 μL reaction containing a final primer concentration of 200 nM and 10 μL of SYBR green buffer solution. Three technical replicates were performed for each reaction. Pipetting was performed using EpMotion 5075 (Eppendorf). The following qPCR protocol was used on the LightCycler 96 (Roche): 3 min of activation phase at 95 °C, 40 cycles of 5 s at 95 °C, and 30 s at 60 °C.

The relative EGFP expression was calculated using the manufacturer's software and the delta−delta Ct method ($2^{-\Delta\Delta Ct}$), with the GAPDH reference gene. To assess differences in the EGFP RNA expression between the treatments with CTRL-effectors and the negative-control effector, statistical analysis was performed using GraphPad Prism 10. Specifically, a one-way ANOVA test was used, followed by the posthoc analysis with a Dunnett's multiple comparisons test and/or a Tukey's multiple comparisons test.

Flow Cytometry and Data Analysis for Protein Repression Assessment. Fluorescence knockdown was assessed using flow cytometry on the BioRad S3e cell sorter system. To prepare cells for analysis, transfected HEK293T cells were washed with 250 μL PBS pH 7.4 (Gibco 10010031), all media was removed, and then 40 μL of Accumax (VWR AM105) was added to the well. 227 μL of cold PBS (pH 7.4) was added to the wells, and cells were resuspended before being transferred to a cell strainer (Corning 352235). Cells were then assessed on the S3e cell sorter with a count of 80,000 cells per sample. Flow cytometry data were analyzed using Floreada.io (https://floreada.io/) (Figure S9).

Library Preparation for High-Throughput Sequencing and Data Analysis. The plasmids encoding the CTRL-effectors (dDiCas7−11, Cas7.1, Cas7.1−7.2, DiCas7−11ΔCas7.1) and CTRL-3′2xmDR-SpyCas9-NG with HEK293-site-3 sgRNA were transiently transfected into HEK293T cells at a molar ratio of 15:1. Subsequent genomic DNA extraction and amplification of the sequencing amplicon was conducted according to Osgood and Zawalick et al. (2025). Briefly, the media was removed 72 h after transfection, the cells were washed with PBS, and then lysed with 100 μL of freshly made lysis buffer (at a 200 μL scale: 196.75 μL H2O, 2 μL Tris−EDTA, 1 μL 1%SDS, 0.25 μL Proteinase K enzyme [Thermo #EO0491]) per confluent well (of a 48-well plate). The amount of lysis buffer was adjusted based on the cell confluency of each well (100 μL for fully confluent wells). The cells were incubated in the lysis buffer for 5 min, then resuspended and removed from the well into PCR tubes. The following thermocycler protocol was used for cell lysis: (a) 1 h at 37 °C; (b) 30 min at 80 °C; (c) ramp to 12 °C. The lysed cells were stored at 4 °C. The lysis (1−2 μL) was used as the template ibxing with Illumina primers with unique barcodes. Round 2 PCR was completed using Phusion High-Fidelity DNA Polymerase (NEB #M0530L) for 9 cycles of amplification. After determining the relative concentration of each sample using gel electrophoresis, concentrations were normalized by pooling 1−10 μL of each round 2 PCR product and then purified with the Monarch Gel Extraction Kit (NEB #T1020) based on the manufacturer's protocol. The purified samples were sequenced with a 300-cycle paired-end NGS run on a MiniSeq high-throughput DNA sequencer (Illumina).[44]

Sequencing reads were demultiplexed using MiniSeq Reporter (Illumina), and FASTQ files were analyzed with CRISPResso2.[45] CRISPRessoBatch was used to analyze and compare multiple experimental conditions at the same site, which generated the indel frequency of each sample within the same quantification window (8-bp sequences that flank both sides of the predicted cleavage site) (Table S4).

■ ASSOCIATED CONTENT

Data Availability Statement

Complete sequence maps and plasmids are deposited to Addgene.org (constructs with Addgene ID in Figure S1 and a full list of plasmids with Addgene ID in Table S5). All data used to generate figures are provided in the Supporting Information/Tables.

Supporting Information

The Supporting Information is available free of charge at https://pubs.acs.org/doi/10.1021/acssynbio.5c00658.

Additional experimental details, construct architecture, sequences, and raw data (PDF)

Table S3_ ANOVA and posthoc tests data.xlsx (XLSX)

Table S4_ The raw data of NGS results for the CTRL-SpyCas9-NG assay.xlsx (XLSX)

Table S5_ The complete list of plasmids used in this study with Addgene ID.xlsx (XLSX)

■ AUTHOR INFORMATION

Corresponding Author

Omar S. Akbari − *School of Biological Sciences, Department of Cell and Developmental Biology, University of California, San Diego, La Jolla, California 92093, United States;* orcid.org/0000-0002-6853-9884; Phone: 858-246-0640; Email: oakbari@ucsd.edu

Authors

Tianqi Wang − *School of Biological Sciences, Department of Cell and Developmental Biology, University of California, San Diego, La Jolla, California 92093, United States;* orcid.org/0000-0002-1460-1013

Daniel J. Brogan − *School of Biological Sciences, Department of Cell and Developmental Biology, University of California, San Diego, La Jolla, California 92093, United States*

Natalie M. Zawalick − *Department of Chemistry and Biochemistry, University of California San Diego, La Jolla, California 92092, United States*

Fangying Chen − *School of Biological Sciences, Department of Cell and Developmental Biology, University of California, San Diego, La Jolla, California 92093, United States*

Yeran Mkrtchian − *School of Biological Sciences, Department of Cell and Developmental Biology, University of California, San Diego, La Jolla, California 92093, United States*

Alexis C. Komor − *Department of Chemistry and Biochemistry, University of California San Diego, La Jolla, California 92092, United States; Moores UCSD Cancer Center, University of California San Diego, La Jolla, California 92093, United States; Sanford Stem Cell Institute, University of California San Diego, La Jolla, California 92037, United States;* orcid.org/0000-0001-5043-0998

Complete contact information is available at: https://pubs.acs.org/10.1021/acssynbio.5c00658

Author Contributions

DJB conceptualized the study. TW and DJB designed experiments. TW performed all cell-based and molecular experiments and NMZ performed all NGS assays. TW and FC performed data and statistical analysis. TW and YM developed

https://doi.org/10.1021/acssynbio.5c00658
ACS Synth. Biol. XXXX, XXX, XXX−XXX

constructs for all assays. OSA and ACK guided experimental design and data analysis. OSA, ACK, DJB, TW, NMZ, and FC contributed to writing and editing the final manuscript.

Funding

This work was supported by funding from NIH awards (R01AI19001−01, R21RAI149161A and DP2AI152071) awarded to OSA. ACK and NMZ were supported by the NIH through grant no. R35GM138317 (awarded to ACK). Figures were created using Prism10 for macOS (GraphPad Software, San Diego, USA) and www.BioRender.com.

Notes

The authors declare the following competing financial interest(s): A patent has been filed pertaining to the technology reported in this study. O.S.A. is a founder of Agragene, Inc. and Synvect, Inc., with equity interest. The terms of this arrangement have been reviewed and approved by the University of California, San Diego in accordance with its conflict of interest policies. A.C.K. is an equity holder for Pairwise Plants and Beam Therapeutics, and receives royalties from Pairwise Plants, Beam Therapeutics, and Editas Medicine via patents licensed from Harvard University. D.J.B is currently an employee at Arbor Biotechnologies.

■ ACKNOWLEDGMENTS

We thank Mallory Evanoff (from Alexis Komor's lab) for advice in NGS data analysis and for providing template plasmids essential to experimentation. Also, we thank Yuko Sugiyama (from Brain Zid's lab) and Ben Pollak (from Alexis Komor's lab) for help with flow cytometry.

■ REFERENCES

(1) Makarova, K. S.; Wolf, Y. I.; Iranzo, J.; Shmakov, S. A.; Alkhnbashi, O. S.; Brouns, S. J. J.; Charpentier, E.; Cheng, D.; Haft, D. H.; Horvath, P.; Moineau, S.; Mojica, F. J. M.; Scott, D.; Shah, S. A.; Siksnys, V.; Terns, M. P.; Venclovas, C.ˇ; White, M. F.; Yakunin, A. F.; Yan, W.; Zhang, F.; Garrett, R. A.; Backofen, R.; van der Oost, J.; Barrangou, R.; Koonin, E. V. Evolutionary Classification of CRISPR−Cas Systems: A Burst of Class 2 and Derived Variants. *Nat. Rev. Microbiol.* **2020**, *18* (2), 67−83.

(2) Hale, C. R.; Cocozaki, A.; Li, H.; Terns, R. M.; Terns, M. P. Target RNA Capture and Cleavage by the Cmr Type III-B CRISPR−Cas Effector Complex. *Genes Dev.* **2014**, *28* (21), 2432.

(3) Liu, T. Y.; Liu, J.-J.; Aditham, A. J.; Nogales, E.; Doudna, J. A. Target Preference of Type III-A CRISPR-Cas Complexes at the Transcription Bubble. *Nat. Commun.* **2019**, *10* (1), 3001−3013.

(4) O'Connell, M. R. Molecular Mechanisms of RNA Targeting by Cas13-Containing Type VI CRISPR-Cas Systems. *J. Mol. Biol.* **2019**, *431* (1), 66.

(5) Colognori, D.; Trinidad, M.; Doudna, J. A. Precise Transcript Targeting by CRISPR-Csm Complexes. *Nat. Biotechnol.* **2023**, *41* (9), 1256−1264.

(6) Özcan, A.; Krajeski, R.; Ioannidi, E.; Lee, B.; Gardner, A.; Makarova, K. S.; Koonin, E. V.; Abudayyeh, O. O.; Gootenberg, J. S. Programmable RNA Targeting with the Single-Protein CRISPR Effector Cas7−11. *Nature* **2021**, *597* (7878), 720−725.

(7) Abudayyeh, O. O.; Gootenberg, J. S.; Essletzbichler, P.; Han, S.; Joung, J.; Belanto, J. J.; Verdine, V.; Cox, D. B. T.; Kellner, M. J.; Regev, A.; Lander, E. S.; Voytas, D. F.; Ting, A. Y.; Zhang, F. RNA Targeting with CRISPR−Cas13. *Nature* **2017**, *550* (7675), 280−284.

(8) Smargon, A. A.; Cox, D. B. T.; Pyzocha, N. K.; Zheng, K.; Slaymaker, I. M.; Gootenberg, J. S.; Abudayyeh, O. A.; Essletzbichler, P.; Shmakov, S.; Makarova, K. S.; Koonin, E. V.; Zhang, F. Cas13b Is a Type VI-B CRISPR-Associated RNA-Guided RNAse Differentially Regulated by Accessory Proteins Csx27 and Csx28. *Mol. cell* **2017**, *65* (4), 618.

(9) No title]. https://www.cell.com/cell/pdf/S0092-8674(18)30207-1.pdf (accessed Oct 29, 2024).

(10) Wessels, H. H.; Méndez-Mancilla, A.; Guo, X.; Legut, M.; Daniloski, Z.; Sanjana, N. E. Massively Parallel Cas13 Screens Reveal Principles for Guide RNA Design. *Nat. Biotechnol.* **2020**, *38* (6), 722.

(11) Kuo, H.-C.; Prupes, J.; Chou, C.-W.; Finkelstein, I. J. Massively Parallel Profiling of RNA-Targeting CRISPR-Cas13d. *Nat. Commun.* **2024**, *15* (1), 498.

(12) Gootenberg, J. S.; Abudayyeh, O. O.; Lee, J. W.; Essletzbichler, P.; Dy, A. J.; Joung, J.; Verdine, V.; Donghia, N.; Daringer, N. M.; Freije, C. A.; Myhrvold, C.; Bhattacharyya, R. P.; Livny, J.; Regev, A.; Koonin, E. V.; Hung, D. T.; Sabeti, P. C.; Collins, J. J.; Zhang, F. Nucleic Acid Detection with CRISPR-Cas13a/C2c2. *Science* **2017**, *356* (6336), 438.

(13) Gootenberg, J. S.; Abudayyeh, O. O.; Kellner, M. J.; Joung, J.; Collins, J. J.; Zhang, F. Multiplexed and Portable Nucleic Acid Detection Platform with Cas13, Cas12a, and Csm6. *Science* **2018**, *360*, 439.

(14) Brogan, D. J.; Chaverra-Rodriguez, D.; Lin, C. P.; Smidler, A. L.; Yang, T.; Alcantara, L. M.; Antoshechkin, I.; Liu, J.; Raban, R. R.; Belda-Ferre, P.; Knight, R.; Komives, E. A.; Akbari, O. S. Development of a Rapid and Sensitive CasRx-Based Diagnostic Assay for SARS-CoV-2. *ACS Sens.* **2021**, *6*, 3957.

(15) Buchman, A. B.; Brogan, D. J.; Sun, R.; Yang, T.; Hsu, P. D.; Akbari, O. S. Programmable RNA Targeting Using CasRx in Flies. *CRISPR J.* **2020**, *3* (3), 164.

(16) Li, Y.; Xu, J.; Guo, X.; Li, Z.; Cao, L.; Liu, S.; Guo, Y.; Wang, G.; Luo, Y.; Zhang, Z.; Wei, X.; Zhao, Y.; Liu, T.; Wang, X.; Xia, H.; Kuang, M.; Guo, Q.; Li, J.; Chen, L.; Wang, Y.; Li, Q.; Wang, F.; Liu, Q.; You, F. The Collateral Activity of RfxCas13d Can Induce Lethality in a RfxCas13d Knock-in Mouse Model. *Genome Biol.* **2023**, *24* (1), 20−25.

(17) Wu, Q.-W.; Kapfhammer, J. P. The Bacterial Enzyme Cas13 Interferes with Neurite Outgrowth from Cultured Cortical Neurons. *Toxins* **2021**, *13* (4), 262.

(18) Wang, Q.; Liu, X.; Zhou, J.; Yang, C.; Wang, G.; Tan, Y.; Wu, Y.; Zhang, S.; Yi, K.; Kang, C. The CRISPR-Cas13a Gene-Editing System Induces Collateral Cleavage of RNA in Glioma Cells. *Adv. Sci.* **2019**, *6* (20), 1901299.

(19) East-Seletsky, A.; O'Connell, M. R.; Knight, S. C.; Burstein, D.; Cate, J. H. D.; Tjian, R.; Doudna, J. A. Two Distinct RNase Activities of CRISPR-C2c2 Enable Guide-RNA Processing and RNA Detection. *Nature* **2016**, *538* (7624), 270−273.

(20) Zhang, B.; Ye, Y.; Ye, W.; Perčulija, V.; Jiang, H.; Chen, Y.; Li, Y.; Chen, J.; Lin, J.; Wang, S.; Chen, Q.; Han, Y.-S.; Ouyang, S. Two HEPN Domains Dictate CRISPR RNA Maturation and Target Cleavage in Cas13d. *Nat. Commun.* **2019**, *10* (1), 2544.

(21) Zhang, C.; Konermann, S.; Brideau, N. J.; Lotfy, P.; Wu, X.; Novick, S. J.; Strutzenberg, T.; Griffin, P. R.; Hsu, P. D.; Lyumkis, D. Structural Basis for the RNA-Guided Ribonuclease Activity of CRISPR-Cas13d. *Cell* **2018**, *175* (1), 212−223.e17.

(22) Kick, L. M.; von Wrisberg, M.-K.; Runtsch, L. S.; Schneider, S. Structure and Mechanism of the RNA Dependent RNase Cas13a from Rhodobacter Capsulatus. *Commun. Biol.* **2022**, *5* (1), 71.

(23) Kato, K.; Zhou, W.; Okazaki, S.; Isayama, Y.; Nishizawa, T.; Gootenberg, J. S.; Abudayyeh, O. O.; Nishimasu, H. Structure and Engineering of the Type III-E CRISPR-Cas7−11 Effector Complex. *Cell* **2022**, *185* (13), 2324−2337.

(24) Burris, B. J. D.; Molina Vargas, A. M.; Park, B. J.; O'Connell, M. R. Optimization of Specific RNA Knockdown in Mammalian Cells with CRISPR-Cas13. *Methods* **2022**, *206*, 58−68.

(25) van Beljouw, S. P. B.; Haagsma, A. C.; Rodríguez-Molina, A.; van den Berg, D. F.; Vink, J. N. A.; Brouns, S. J. J. The gRAMP CRISPR-Cas Effector Is an RNA Endonuclease Complexed with a Caspase-like Peptidase. *Science* **2021**, *373*, 1349.

(26) DiAndreth, B.; Wauford, N.; Hu, E.; Palacios, S.; Weiss, R. PERSIST Platform Provides Programmable RNA Regulation Using CRISPR endoRNases. *Nat. Commun.* **2022**, *13* (1), 2582.

https://doi.org/10.1021/acssynbio.5c00658
ACS Synth. Biol. XXXX, XXX, XXX−XXX

(27) Niewoehner, O.; Jinek, M.; Doudna, J. A. Evolution of CRISPR RNA Recognition and Processing by Cas6 Endonucleases. *Nucleic Acids Res.* **2014**, *42* (2), 1341.

(28) Carte, J.; Wang, R.; Li, H.; Terns, R. M.; Terns, M. P. Cas6 Is an Endoribonuclease That Generates Guide RNAs for Invader Defense in Prokaryotes. *Genes Dev.* **2008**, *22* (24), 3489−3496.

(29) Goswami, H. N.; Rai, J.; Das, A.; Li, H. Molecular Mechanism of Active Cas7−11 in Processing CRISPR RNA and Interfering Target RNA. *Elife* **2022**, *11*, No. e81678.

(30) Mugridge, J. S.; Coller, J.; Gross, J. D. Structural and Molecular Mechanisms for the Control of Eukaryotic 5′-3′ mRNA Decay. *Nat. Struct. Mol. Biol.* **2018**, *25* (12), 1077−1085.

(31) Lin, C. P.; Li, H.; Brogan, D. J.; Wang, T.; Akbari, O. S.; Komives, E. A. CRISPR RNA Binding Drives Structural Ordering That Primes Cas7−11 for Target Cleavage. *bioRxivorg* **2024**.

(32) Brogan, D. J.; Benetta, E. D.; Wang, T.; Lin, C. P.; Chen, F.; Li, H.; Lin, C.; Komives, E. A.; Akbari, O. S. Synthetic Type III-E CRISPR-Cas Effectors for Programmable RNA-Targeting. *bioRxiv* **2024**.

(33) Huo, Y.; Zhao, H.; Dong, Q.; Jiang, T. Cryo-EM Structure and Protease Activity of the Type III-E CRISPR-Cas Effector. *Nat. Microbiol.* **2023**, *8* (3), 522−532.

(34) Nishimasu, H.; Shi, X.; Ishiguro, S.; Gao, L.; Hirano, S.; Okazaki, S.; Noda, T.; Abudayyeh, O. O.; Gootenberg, J. S.; Mori, H.; Oura, S.; Holmes, B.; Tanaka, M.; Seki, M.; Hirano, H.; Aburatani, H.; Ishitani, R.; Ikawa, M.; Yachie, N.; Zhang, F.; Nureki, O. Engineered CRISPR-Cas9 Nuclease with Expanded Targeting Space. *Science* **2018**, *361* (6408), 1259−1262.

(35) Konermann, S.; Lotfy, P.; Brideau, N. J.; Oki, J.; Shokhirev, M. N.; Hsu, P. D. Transcriptome Engineering with RNA-Targeting Type VI-D CRISPR Effectors. *Cell* **2018**, *173* (3), 665−676.

(36) Komor, A. C.; Kim, Y. B.; Packer, M. S.; Zuris, J. A.; Liu, D. R. Programmable Editing of a Target Base in Genomic DNA without Double-Stranded DNA Cleavage. *Nature* **2016**, *533* (7603), 420−424.

(37) Teixeira, A. P.; Fussenegger, M. Synthetic Gene Circuits for Regulation of Next-Generation Cell-Based Therapeutics. *Advanced Science* **2023**, *11* (8), 2309088.

(38) Santos-Moreno, J.; Schaerli, Y. CRISPR-Based Gene Expression Control for Synthetic Gene Circuits. *Biochem. Soc. Trans.* **2020**, *48* (5), 1979.

(39) Chen, W. C. W.; Gaidukov, L.; Lai, Y.; Wu, M.-R.; Cao, J.; Gutbrod, M. J.; Choi, G. C. G.; Utomo, R. P.; Chen, Y.-C.; Wroblewska, L.; Kellis, M.; Zhang, L.; Weiss, R.; Lu, T. K. A Synthetic Transcription Platform for Programmable Gene Expression in Mammalian Cells. *Nat. Commun.* **2022**, *13* (1), 6167.

(40) Engstrom, M. D.; Pfleger, B. F. Transcription Control Engineering and Applications in Synthetic Biology. *Synth. Syst. Biotechnol.* **2017**, *2* (3), 176−191.

(41) Houdebine, L.-M.; Lema, M. A.; Burachik, M. Advances in the Development of Genetically Modified Animals. https://conahcyt.mx/cibiogem/images/cibiogem/comunicacion/publicaciones/CBR-V7/Article2_7.pdf.

(42) Yan, Y.; Hosseini, B.; Scheld, A.; Pasham, S.; Rehling, T.; Schetelig, M. F. Effects of Antibiotics on the in Vitro Expression of Tetracycline-off Constructs and the Performance of Drosophila Suzukii Female-Killing Strains. *Front. Bioeng. Biotechnol.* **2023**, *11*, 876492.

(43) Anzalone, A. V.; Randolph, P. B.; Davis, J. R.; Sousa, A. A.; Koblan, L. W.; Levy, J. M.; Chen, P. J.; Wilson, C.; Newby, G. A.; Raguram, A.; Liu, D. R. Search-and-Replace Genome Editing without Double-Strand Breaks or Donor DNA. *Nature* **2019**, *576* (7785), 149−157.

(44) Osgood, N. R. B.; Zawalick, N. M.; Sawyer, C. B.; Cowan, Q. T.; Gu, S.; Mawson, S. J.; Ranzau, B. L.; Li, L.; Gymrek, M.; Goren, A.; Komor, A. C. Genome Editing with Programmable Base Editors in Human Cells. *Methods Enzymol.* **2025**, *712*, 351−404.

(45) Clement, K.; Rees, H.; Canver, M. C.; Gehrke, J. M.; Farouni, R.; Hsu, J. Y.; Cole, M. A.; Liu, D. R.; Joung, J. K.; Bauer, D. E.; Pinello, L. CRISPResso2 Provides Accurate and Rapid Genome Editing Sequence Analysis. *Nat. Biotechnol.* **2019**, *37* (3), 224−226.

https://doi.org/10.1021/acssynbio.5c00658
ACS Synth. Biol. XXXX, XXX, XXX−XXX